PFC/JA-86-51

Generation of Electromagnetic Radiation From A Drifting and Rotating Electron Ring In A Rippled Magnetic Field

Yuan-Zhao Yin,* Run-Jie Ying,* and G. Bekefi

September 1986

Plasma Fusion Center
Massachusetts Institute of Technology
Cambridge, Massachusetts 02139 USA

This work was supported in part by the U.S. Department of Energy and in part by the U.S. Air Force Office of Scientific Research.

Submitted for publication to Special Issue of the IEEE Journal of Quantum Electronics on Free-Electron Lasers

*Present address: Institute of Electronics, Academia Sinica, Beijing, The People's Republic of China

GENERATION OF ELECTROMAGNETIC RADIATION FROM A DRIFTING AND ROTATING ELECTRON RING IN A RIPPLED MAGNETIC FIELD

Yuan-Zhao Yin, Run-Jie Ying
Institute of Electronics, Academia Sinica
Beijing, The People's Republic of China

and

G. Bekefi
Department of Physics and Research Laboratory of Electronics
Massachusetts Institute of Technology
Cambridge, Massachusetts 02139 U.S.A.

Coherent electromagnetic radiation from a thin rotating annular ring of relativistic electrons with axial drift, and confined between concentric cylinders comprising a coaxial waveguide, is studied theoretically. The electrons are assumed to move in quasihelical orbits under the combined action of a uniform axial magnetic field and an azimuthally periodic wiggler magnetic field. The instability analysis is based on the linearized Vlasov-Maxwell equations for the perturbations about a self-consistent beam equilibrium. The dispersion equations for the transverse magnetic ($TM_{\ell,m}$) modes are derived and analyzed. Coherent radiation occurs near frequencies ω corresponding to the crossing points of the electromagnetic modes $\omega^2=c^2k_{\|}^2+\omega_c^2(\ell,m)$ and the beam modes $\omega=v_{\|}k_{\|}+(\ell+N)\Omega_{\|}$, where ω_c and $\Omega_{\|}$ are the waveguide cutoff frequency and the electron cyclotron frequency, respectively, $v_{\|}$ is the axial drift velocity of electrons, $k_{\|}$ is the wavenumber of the electromagnetic wave along the axis, and N is the number of wiggler periods along the azimuth.

I. INTRODUCTION

Numerous theoretical[1] and experimental[2] studies have been carried out of free-electron lasers (FEL's) in linear geometry with spatially periodic transverse[1,2] or longitudinal[3-6] magnetic wiggler fields. Such configurations have gain limitations imposed by the finite length of the interaction region. Recently, a novel circular version of the free-electron laser has been explored both theoretically,[7-13] and experimentally[14-17] in which a rotating, relativistic electron stream is subjected to an azimuthally periodic wiggler field superimposed on the axial guiding magnetic field. The potential advantages of circular FEL's as compared with the coventional linear form are several. First, the beam circulates continuously through the wiggler field resulting in a long effective interaction region. Second, because of the recirculation of the growing electromagnetic wave, the device provides its own internal feedback and is in essence an oscillator rather than an amplifier, as is the case in linear FEL's. Third, because the electron motion is primarily circular, the system is very compact. Lastly, theory[11,12] indicates that a circular FEL can have a much larger bandwidth than a corresponding linear version.

In our previous theoretical article[10] we assumed that the rotating beam has no axial drift velocity and the coaxial waveguide was under cutoff conditions. In fact, some drift velocity always exists in the experiments, and, as we will show, this affects considerably the operation of the FEL.

In this paper we remove the above two assumptions. Besides, because of the energy spread of the rotating beam, the electrons occupy different radii in the uniform guiding magnetic field. Therefore, we also remove the assumption of the infinitely thin beam of the previous paper[10] and let the beam have finite but very small thickness. The instability analysis is based on the linearized Vlasov-Maxwell equations for perturbations about a self-consistent beam equilibrium. Section II contains a description of the configuration, and

an analysis of the beam dynamics. Section III contains the derivation of the dispersion relations for the transverse magnetic ($TM_{\ell,m}$) modes excited by the electron ring confined in a coaxial waveguide system. In Sec. IV we present examples of computer generated solutions of the dispersion equations, and finally Sec. V contains a discussion of the results.

We will show that growing electromagnetic fields occur near frequencies corresponding to the crossing points of the $TM_{\ell,m}$ waveguide modes, $\omega^2 = c^2k_{\parallel}^2+\omega_c^2(\ell,m)$, and the beam modes $\omega=v_{\parallel}k_{\parallel}+(\ell+N)\Omega_{\parallel}$, where ω_c is the waveguide cutoff frequency, $\Omega_{\parallel}$ is the electron cyclotron frequency, $k_{\parallel}$ is the wavenumber of the electromagnetic waves along the axis, $v_{\parallel}$ is the axial drifting velocity of electrons, and N is the number of wiggler periods around the circumference.

II. ELECTRON MOTION AND EQUILIBRIUM DISTRIBUTION IN THE GUIDE AND WIGGLER FIELDS

In our model, an annular electron ring of finite but very small thickness rotates within the gap formed by two concentric grounded metal cylinders of radii a and b, as is illustrated in Fig. 1. The two cylinders form a coaxial waveguide. The electron ring is confined by a uniform axial magnetic field $B_{\parallel}\hat{z}$ directed along the waveguide axis.

Superimposed on the axial magnetic field $B_{\parallel}\hat{z}$ is an azimuthally periodic wiggler field $\bar{B}_w$ (Fig. 1) which perturbs the electron stream. Subject to the requirement that $\nabla\cdot\bar{B}_w=\nabla\times\bar{B}_w=0$ the field in the vacuum gap between the concentric cylinders a,b is calculated to be[14]

$$\bar{B}_w = \hat{r}\,\frac{B_{ow}}{2}\cos(N\theta)\left[\left(\frac{r}{a}\right)^{N-1} + \left(\frac{b}{r}\right)^{N+1}\right]\left(\frac{a}{b}\right)^{(N^2-1)/2N}$$
$$- \hat{\theta}\,\frac{B_{ow}}{2}\sin(N\theta)\left[\left(\frac{r}{a}\right)^{N-1} - \left(\frac{b}{r}\right)^{N+1}\right]\left(\frac{a}{b}\right)^{(N^2-1)/2N} \qquad (1)$$

where $\hat{r}$ and $\hat{\theta}$ are unit vectors in the radial and azimuthal directions, respectively. Here $N=\pi(a+b)/\ell_0$ is the number of spatial periods and ℓ_0 is the linear periodicity defined midway in the gap; B_{0w} is the amplitude of the radial component of field at a distance $r=R_0\equiv\left(a^{N-1}b^{N+1}\right)^{1/(2N)}$ where the azimuthal field component vanishes (which is roughly midway between the cylinders). We see that near the center of the gap the wiggler field is primarily radial and is thus transverse to the electron flow velocity, as is the case in conventional free-electron lasers. The undulatory force $-e(\bar{v}/c)\times\bar{B}_w$ is along the $\pm z$ axis. We shall find in Sec. III that this undulatory motion gives rise to a z-directed rf current which excites growing transverse magnetic ($TM_{\ell,m}$) waveguide modes.

To simplify computations we shall assume henceforth that the center of the electron ring is at a radius which coincides exactly (or nearly so) with the radius $R_0\equiv\left(a^{N-1}b^{N+1}\right)^{1/(2N)}$ discussed above. Under these conditions the $\hat{\theta}$ component of $\bar{B}_w$ can be neglected, and $\bar{B}_w$ of Eq. (1) becomes

$$\bar{B}_w = \hat{r}B_{0w}\cos(N\theta). \tag{2}$$

We shall now assume a sufficiently weak pump field such that

$$f \equiv |\Omega_w/N\Omega_{\parallel}| << 1 . \tag{3}$$

Here $\Omega_w=eB_{0w}/m_0c\gamma_0$ is the cyclotron frequency associated with the wiggler field and $\Omega_{\parallel}=eB_{\parallel}/m_0c\gamma_0$ is the cyclotron frequency associated with the axial-guide field. Another assumption is that the electron beam is tenuous with negligibly small equilibrium self fields. Subject to these assumptions the motion of electrons in the absence of RF fields is characterized by four single-particle constants of the motion. These are

$$
\begin{aligned}
p^2 &= p_r^2 + p_\theta^2 + p_z^2 \\
C_z &= P_z - m_0\gamma_0 f r\Omega_{\parallel} \sin(N\theta) \\
C_\theta &= r\left(P_\theta - \tfrac{1}{2} m_0\gamma_0 r\Omega_{\parallel}\right) + m_0\gamma_0 f v_{\parallel} r \sin(N\theta) - \tfrac{1}{4} m_0\gamma_0 f^2\Omega_{\parallel} r^2 \sin(2N\theta) \\
P_r &= 0
\end{aligned}
\tag{4}
$$

where P_r, P_θ and P_z are the radial, azimuthal and axial momenta, respectively, $\gamma_0=(1-\beta_0^2)^{-\frac{1}{2}}=1+eV/m_0c^2$ is the relativistic energy factor, $\beta_0^2=\beta_\theta^2+\beta_{\parallel}^2$, $\beta_0=v_0/c$, $\beta_\theta=v_\theta/c$, $\beta_{\parallel}=v_{\parallel}/c$, eV is the kinetic energy, -e is the electron charge, m_0 is the electron rest mass, and c is the speed of light in vacuo. In the derivation we have assumed that the axial velocity is small compared with the azimuthal velocity so that,

$$\frac{v_{\parallel}}{R_0\Omega_{\parallel}} \ll 1. \tag{5}$$

The TM-mode stability analysis in the next section is carried out for perturbations about the self-consistent equilibrium distribution given by

$$f_b^0(P,C_z,C_\theta,P_r) = n_0 R_0 \Theta\left[\Delta^2 - (P-\gamma_0 m_0 v_0)^2\right]\delta(P_r)\delta(C_\theta-P_0)\delta(C_z-m_0\gamma_0 v_{\parallel}) \tag{6}$$

where $P_0= (e/2c)B_{\parallel}(R_0^2+a_0^2)$, $v_0^2=v_{\parallel}^2+R_0^2\Omega_{\parallel}^2$, n_0 is the density of electrons, Δ is the momentum spread, and $2a_0$ is the thickness of the electron ring assumed to be sufficiently thin so that,

$$R_0 \gg a_0. \tag{7}$$

The parameter

$$\Theta(x) = \begin{cases} 1 & x \geq 0 \\ 0 & x < 0 \end{cases}$$

is the Heaviside step function.

It readily follows that the radial, azimuthal, and axial momenta of the beam electrons averaged over the entire distribution of momenta, are

$$\langle P_r \rangle = 0$$
$$\langle P_\theta \rangle \simeq m_0\gamma_0 R_0\Omega_{\parallel} \tag{8}$$
$$\langle P_z \rangle = m_0\gamma_0[v_{\parallel} + fr\Omega_{\parallel}\sin(N\theta)].$$

Moreover, it can be shown from Eqs. (3), (5), and (6) that $f_b^0(P,C_z,C_\theta,P_r)$ corresponds to a sharp-boundary equilibrium with a density profile $n_b^0(r)=\int d^3P f_b^0$ given by

$$n_b^0(r) = \begin{cases} n_0 = \text{const.}, & -a_0 \lesssim r - R_0 \lesssim a_0 \\ 0 \quad , & \text{otherwise .} \end{cases} \tag{9}$$

Here, the half thickness of the electron ring is defined by

$$a_0 = \frac{\Delta}{\gamma_0 m_0 \Omega_{\parallel}} \quad . \tag{10}$$

The equations of motion for an electron moving in the wiggler field described by Eq. (2) and the axial-guide field $B_{\parallel}\hat{z}$ are given by

$$\frac{dP_r}{dt} - P_\theta \frac{v_\theta}{r} = -\frac{eB_{\parallel}}{c} v_\theta$$
$$\frac{dP_\theta}{dt} + P_r \frac{v_\theta}{r} = -\frac{eB_{0w}}{c} v_z \cos(N\theta) + \frac{eB_{\parallel}}{c} v_r \tag{11}$$
$$\frac{dP_z}{dt} = \frac{eB_{0w}}{c} v_\theta \cos(N\theta).$$

Letting $\tau = t'-t$ and solving Eqs. (11), we obtain,

$$v_z' = v_z - fr\Omega_{\parallel}\sin(N\theta) + fr\Omega_{\parallel}\sin\left(N\frac{v_\theta}{r}\tau + N\theta\right)$$
$$v_\theta' = v_\theta + fv_{\parallel}\sin(N\theta) - fv_{\parallel}\sin\left(N\frac{v_\theta}{r}\tau + N\theta\right) - \frac{1}{4}f^2 r\Omega_{\parallel}\cos(2N\theta) \tag{12}$$
$$+ \frac{1}{4}f^2 r\Omega_{\parallel}\cos\left(2N\frac{v_\theta}{r}\tau + 2N\theta\right) \simeq v_\theta$$
$$v_r' = 0$$

and,

$$z' = z + v_z\tau + f\frac{r}{N}\cos(N\theta) - f\frac{r}{N}\cos\left(N\frac{v_\theta}{r}\tau + N\theta\right) - fr\Omega_{\parallel}\sin(N\theta)\tau$$

$$\theta' = \theta + \frac{v_\theta}{r}\tau \qquad (13)$$

$$r' = r \ .$$

When $t'=t$, the electron trajectory $(\bar{x}',\bar{P}')$ passes through the phase space point $(\bar{x},\bar{P})$, that is, $v_r'=0$, $v_\theta'=v_\theta$, $v_z'=v_z$, $\theta'=\theta$, $r'=r$, $z'=z$.

III. DISPERSION RELATIONS

In the case of a very tenuous electron ring where all DC and RF space charge fields are neglected (which is the assumption made in this and our earlier[10] paper), the coaxial waveguide modes can be approximated by the unperturbed vacuum transverse electric (TE) and transverse magnetic (TM) modes. Moreover, in this limit the z-directed oscillatory motion caused by the wiggler and given by Eqs. (12) and (13) does not couple to the TE family of modes. Thus, the negative mass instability[10] and the synchronous mode instability[10] which are associated with TE modes do not enter our analysis. This differs from the recent studies of Saito and Wurtele[12,13] who take RF space charge fields into consideration and obtain dispersion equations which contain contributions from the negative mass instability. However, their results are restricted to the case $v_{\parallel}=k_{\parallel}=0$.

In our case the RF fields are then given by

$$E_z^{(1)} = \sum_\ell \tilde{E}_{z\ell}^{(1)}(r)e^{-i(\omega t - k_\parallel z - \ell\theta)} = \sum_\ell C_\ell X_\ell(k_c r)e^{-i(\omega t - k_\parallel z - \ell\theta)}$$

$$E_\theta^{(1)} = \sum_\ell \tilde{E}_{\theta\ell}^{(1)}(r)e^{-i(\omega t - k_\parallel z - \ell\theta)} = -\sum_\ell C_\ell \frac{1}{k_c^2} k_\parallel \ell \frac{1}{r} X_\ell(k_c r)e^{-i(\omega t - k_\parallel z - \ell\theta)}$$

$$E_r^{(1)} = \sum_\ell \tilde{E}_{r\ell}^{(1)}(r)e^{-i(\omega t - k_\parallel z - \ell\theta)} = \sum_\ell C_\ell i \frac{1}{k_c} k_\parallel X'_\ell(k_c r)e^{-i(\omega t - k_\parallel z - \ell\theta)}$$

$$B_z^{(1)} = 0 \tag{14}$$

$$B_\theta^{(1)} = \sum_\ell \tilde{B}_{\theta\ell}^{(1)}(r)e^{-i(\omega t - k_\parallel z - \ell\theta)} = \sum_\ell C_\ell i \frac{1}{k_c^2} \frac{\omega}{c} X'_\ell(k_c r)e^{-i(\omega t - k_\parallel z - \ell\theta)}$$

$$B_r^{(1)} = \sum_\ell \tilde{B}_{r\ell}^{(1)}(r)e^{-i(\omega t - k_\parallel z - \ell\theta)} = \sum_\ell C_\ell \frac{1}{k_c^2} \ell \frac{\omega}{c} \frac{1}{r} X_\ell(k_c r)e^{-i(\omega t - k_\parallel z - \ell\theta)}$$

In the above equations C_ℓ is a constant proportional to the perturbing TM field, and[10]

$$X_\ell(k_c r) = J_\ell(k_c r)N_\ell(k_c a) - J_\ell(k_c a)N_\ell(k_c r) \tag{15}$$

where J_ℓ and N_ℓ are Bessel functions of the first and second kind, respectively; $k_c(\ell,m)$ is the cutoff wave number determined by setting $X_\ell(k_c b)=0$. The cutoff frequency ω_c of the (ℓ,m)th waveguide mode is related to the wave number $k_c(\ell,m)$ through $\omega_c(\ell,m)=ck_c(\ell,m)$; ℓ and m are the azimuthal and radial mode numbers, respectively.

For the equilibrium configuration discussed in Sec. II, we now make use of the linearized Vlasov-Maxwell equations to investigate the stability properties for electromagnetic perturbations with TM-mode polarization. The wave equation for the axial electric field is

$$(\omega^2 - c^2k_\parallel^2 - c^2k_c^2)E_z^{(1)} = -i4\pi\omega J_z^{(1)} \tag{16}$$

where the current density $J_z^{(1)}$ is given by

$$J_z^{(1)} = - e\int d^3p v_z f_b^{(1)}. \tag{17}$$

Making use of the method of characteristics, the linearized Vlasov equation for the perturbed distribution function can be integrated along unperturbed trajectories to yield

$$\hat{f}_b^{(1)}(\vec{x},\vec{p}) = e\int_{-\infty}^{0} d\tau \left[\left[\tilde{E}_{r\ell}^{(1)} - \frac{1}{c} v_z' \tilde{B}_{\theta\ell}^{(1)}\right] \frac{\partial}{\partial p_r'} f_b^0 + \left[\tilde{E}_{\theta\ell}^{(1)} + \frac{1}{c} v_z' \tilde{B}_{r\ell}^{(1)}\right] \frac{\partial}{\partial p_\theta'} f_b^0 \right.$$
$$\left. + \left[\tilde{E}_{z\ell}^{(1)} - \frac{1}{c} v_\theta' \tilde{B}_{r\ell}^{(1)}\right] \frac{\partial}{\partial p_z'} f_b^0\right] e^{-i(\omega\tau - k_\parallel z' - \ell\theta')}. \tag{18}$$

Following the same procedure as we did in the Ref. 18 we obtain, after some tedious algebra, the following dispersion equation:

$$\omega^2 - c^2k_\parallel^2 - c^2k_c^2 = \omega_p^2\omega \frac{2a_0R_0}{D_\ell} X_\ell^2(k_cR_0)$$
$$X \sum_{n=-\infty}^{+\infty} J_n^2\left(k_\parallel f \frac{R_0}{N}\right) \left\{\left(1 - \frac{\Omega_\parallel\omega}{c^2k_c^2}\ell\right)\left(\frac{1}{\Omega_{\ell-nN}} + \frac{v_\parallel k_\parallel}{\Omega_{\ell-nN}^2}\right)\right.$$
$$+ \frac{\ell(\ell-nN)}{k_c^2R_\theta^2} \frac{v_\parallel^2\omega\ell(\ell-nN) - v_\parallel k_\parallel}{c^2\Omega_{\ell-nN}^2}$$
$$\left. + \frac{1}{4} f^2 \frac{\Omega_\parallel\omega}{c^2k_c^2} \ell\left[\frac{[\ell+(n+1)N]\Omega_\parallel + v_\parallel k_\parallel}{\Omega_{\ell+(n+1)N}^2} + \frac{[\ell+(n-1)N]\Omega_\parallel + v_\parallel k_\parallel}{\Omega_{\ell+(n-1)N}^2}\right]\right\} \tag{19}$$

where we have used the middle value theorm for the integrals over r, because with $R_0 >> a_0$,

$$\int_{R_0-a_0}^{R_0+a_0} F(r)dr \cong 2a_0F(R_0). \tag{20}$$

The quatities Ω_ℓ, ω_p, and D_ℓ are given by

$$\Omega_\ell = \omega - v_{\|}k_{\|} - \ell\Omega_{\|}$$

$$\omega_p = (4\pi e^2 n_0/m_0\gamma_0)^{\frac{1}{2}} \tag{21}$$

$$D_\ell = \frac{a^2}{2}X_\ell'(k_c a) - \frac{b^2}{2}X_\ell'(k_c b)$$

The dispersion equation (19) has a very rich harmonic content, and can be solved numerically by retaining several terms in the summation over n. For present purposes, we assume that the harmonics are well separated, and we investigate the stability behavior for n=0 near the resonance,

$$\Omega_{\ell+N} = \omega - v_{\|}k_{\|} - [\ell + N]\Omega_{\|} \cong 0 \tag{22}$$

with the result that,

$$(\omega^2 - c^2k_{\|}^2 - c^2k_c^2)[\omega - v_{\|}k_{\|} - (\ell + N)\Omega_{\|}]^2$$

$$= \frac{1}{4}\omega_p^2 \frac{2a_0R_0}{D_\ell}\frac{\omega^2}{c^2k_c^2} f^2\ell\Omega_{\|}[(\ell+N)\Omega_{\|} + v_{\|}k_{\|}]J_0^2(k_{\|}f\frac{R_0}{N})X_\ell^2(k_cR_0). \tag{23}$$

When $k_{\|}=0$ and $v_{\|}=0$, Eq. (23) becomes

$$(\omega^2 - c^2k_c^2)[\omega - (\ell+N)\Omega_{\|}]^2$$

$$= \frac{1}{4}\omega_p^2 \frac{2a_0R_0}{D_\ell} f^2\ell\Omega_{\|}^2(\ell+N)\ X_\ell^2(k_cR_0) \tag{24}$$

which is found to be very similar to the dispersion equation obtained in our earlier paper[10] based on a fluid model.

IV. NUMERICAL ANALYSIS

From dispersion equation (23) we see that the coupling which causes the instability occurs between the electromagnetic wave and the electron beam wave which, in the absence of the wiggler, have dispersion relations given by

$$\omega^2 = c^2k_{\|}^2 + c^2k_c^2 \tag{25}$$

$$\omega = v_{\|}k_{\|} + (\ell+N)\Omega_{\|}. \tag{26}$$

The crossing point of these two waves corresponds to the case for which their axial phase velocities $\omega/k_{\parallel}$ are equal. Solving Eqs. (25) and (26) we obtain

$$k_{\parallel} = \beta_{\parallel}\gamma_{\parallel}^2 \frac{(\ell+N)\Omega_{\parallel}}{c} \pm \gamma_{\parallel} \frac{1}{c} [\gamma_{\parallel}^2(\ell+N)^2\Omega_{\parallel}^2 - \omega_c^2]^{\frac{1}{2}} \tag{27}$$

$$\omega = \gamma_{\parallel}^2(\ell+N)\Omega_{\parallel} \pm \beta_{\parallel}\gamma_{\parallel}[\gamma_{\parallel}^2(\ell+N)^2\Omega_{\parallel}^2 - \omega_c^2]^{\frac{1}{2}} \tag{28}$$

where

$$\omega_c = ck_c \quad , \quad \gamma_{\parallel} = (1-\beta_{\parallel}^2)^{-\frac{1}{2}} .$$

We see that two waves exist: a high frequency wave and a low frequency wave. However, when

$$\gamma_{\parallel}(\ell+N)\Omega_{\parallel} = \omega_c \tag{29}$$

the axial group velocities $\partial\omega/\partial k_{\parallel}$ of the two waves are equal to the axial electron velocity $v_{\parallel}$. At this "tangential intersection point" there is but one wave

$$k_{\parallel} = \beta_{\parallel}\gamma_{\parallel}^2 \frac{(\ell+N)\Omega_{\parallel}}{c} \tag{30}$$

and

$$\omega = \gamma_{\parallel}^2(\ell+N)\Omega_{\parallel} = \gamma_{\parallel}\omega_c . \tag{31}$$

The instability growth rate is largest at this frequency ω and axial wave number $k_{\parallel}$, as is found from a solution of the complete dispersion equation (23). In all cases the cutoff wave number k_c and the corresponding cutoff frequency ω_c are obtained from a solution of the equation,

$$X_{\ell}(k_c b) = J_{\ell}(k_c b)N_{\ell}(k_c a) - J_{\ell}(k_c a)N_{\ell}(k_c b) = 0 \tag{32}$$

obtained numerically by Muller's method. A less accurate procedure was used in our earlier publication,[10] where an approximate, analytic expression for ω_c was given.

The two-dimensional phase space plot of $k_{\parallel}$ versus ℓ, obtained from Eq. (27), is illustrated in Fig. 2(a). The tangential interaction points are marked by the solid points. Each curve is for a different value of the energy

parameter γ_0. For a certain value of γ_0, the curves reduce to a single point referred to as the "merging point". Here both the axial and azimuthal group velocities of interacting waves given by Eqs. (25) and (26) are equal, that is $(\partial\omega/\partial k_{\parallel})_{\text{wave 1}} = (\partial\omega/k_{\parallel})_{\text{wave 2}}$; $\left(\frac{\partial\omega}{\partial \ell}\right)_{\text{wave 1}} = \left(\frac{\partial\omega}{\partial \ell}\right)_{\text{wave 2}}$. This point is marked in Fig. 2(a) by an asterisk ($*$).

Figure 2(b) shows the instability growth rates (imaginary value of ω) corresponding to the values of ℓ of Fig. 2(a). Only the growth rates for the higher $k_{\parallel}$ values are shown. The growth rates for the lower $k_{\parallel}$ values differ but little from the results shown. The reason is that for our choice of $k_{\parallel}v_{\parallel} << (\ell+N)\Omega_{\parallel}$, small differences in $k_{\parallel}$ have little effect on the growth rate.

Figure 3 illustrates the behavior of the growth rate as a function of ℓ for a fixed value $k_{\parallel}=k_{\parallel}^{*}=2.093\ \text{cm}^{-1}$. With this value of $k_{\parallel}$ one traverses the "merging point" at $\ell\equiv\ell^{*}=57$ [see Fig. 2(a)] and $\gamma_0\equiv\gamma_0^{*}=2.595$. It is seen that the growth rate is maximum at the merging point.

Because of the radial variation of the RF electric fields within the coaxial waveguide, the growth rate is a fairly sensitive function of the radius R_0 of the electron ring.[12] Figure 4 illustrates this effect. In Fig. 4(a) we once again plot the two-dimensional phase space diagram $k_{\parallel}$ versus ℓ, each curve for a different radius R_0. Figure 4(b) gives the corresponding growth rates for the larger of the two $k_{\parallel}$ values. Figure 5 shows the growth rates as a function of R_0 when ℓ is taken as the parameter. For values of R_0 below and above those shown in the figure, there is no wave-particle interaction, and thus no FEL instability. This manifests itself by the sudden termination of the lines.

V. CONCLUSIONS

In this paper we have used the Vlasov-Maxwell equations to analyze the instability of the $TM_{\ell,m}$ modes in a coaxial waveguide. The growing electro-

magnetic waves are excited by a rotating relativistic electron ring moving along the axial direction. The electron ring is thin and tenuous and is subjected to an azimuthally periodic wiggler magnetic field. It is found that radiation growth occurs near frequencies corresponding to the crossing points of the waveguide modes $\omega^2=c^2k_{\parallel}^2+\omega_c^2$ and the beam modes $\omega=v_{\parallel}k_{\parallel}+(\ell+N)\Omega_{\parallel}$, where ω_c is the cutoff frequency of the coaxial waveguide and $\Omega_{\parallel}$ is the electron cyclotron frequency in the axial guiding magnetic field. The coupling occurs in the two-dimensional phase space of $k_{\parallel}$ and ℓ, instead of the one-dimensional phase space, $k_{\parallel}$, as in conventional linear free electron lasers, or in the one-dimensional phase space, ℓ, as in the pure circular free electron lasers,[10] with $k_{\parallel}=0$.

The numerical results shown in Figs. 2 to 5 are for the special case of a six-period azimuthal wiggler (N=6), and for the lowest radial waveguide mode (m=1). The results for higher N and m are found to be similar to those shown. The instability growth rates are in all cases highest at the "merging point" $\ell=\ell^*$, $k_{\parallel}=k_{\parallel}^*$, $\gamma_0=\gamma_0^*$. Table I lists the growth rates and the corresponding radiation frequencies at the merging points for three different wiggler periodicities N.

ACKNOWLEDGEMENTS

This work was supported in part by the U.S. Department of Energy and in part by the U.S. Air Force Office of Scientific Research.

REFERENCES

1. N.M. Kroll and W.A. McMullin, Phys. Rev. A17, 300 (1978); P. Sprangle, and R.A. Smith, ibid. 21, 293 (1980), and references therein.
2. P.A. Sprangle, R.A. Smith, and V.L. Granatstein in Infrared and Submillimeter Waves, edited by K. Button (Academic, New York, 1979) Vol. 1, p. 279 and references therein.
3. W.A. McMullin and G. Bekefi, Appl. Phys. Lett. 39, 845 (1981).
4. W.A. McMullin and G. Bekefi, Phys. Rev. A25, 1826 (1982).
5. R.C. Davidson and W.A. McMullin, Phys. Rev. A26, 1997 (1982).
6. R.C. Davidson and W.A. McMullin, Phys. Fluids 26, 840 (1983).
7. G. Bekefi, Appl. Phys. Lett. 40, 578 (1982).
8. R.C. Davidson, W.A. McMullin, and K. Tsang, Phys. Fluids 27, 233 (1984).
9. C.L. Chang, E. Ott, T.M. Antonsen, Jr., and A.T. Drobot, Phys. Fluids, 27, 2937 (1984).
10. Y.Z. Yin and G. Bekefi, Phys. Fluids 28, 1186 (1985).
11. L.S. Schultz, E. Ott, T.M. Antonsen, Bull. Am. Phys. Soc. 30, 1549 (1985).
12. H. Saito and J.S, Wurtele, 10th International Conference Infrared and Millimeter Waves, December 1985, Lake Buena Vista, Florida.
13. H. Saito and J.S. Wurtele (to be published).
14. G. Bekefi, R.E. Shefer, and B.D. Nevins, Lasers '82 Conference, Proc. of the Society for Optical and Quantum Electronics (SOQUE, New Orleans, Louisiana, 1982) p. 136.
15. G. Bekefi, R.E. Shefer, and W.W. Destler, Appl. Phys. Lett. 44, 280 (1984).
16. W.W. Destler, F.M. Aghamir, D.A. Boyd, G. Bekefi, R.E. Shefer, and Y.Z. Yin, Phys. Fluids 28, 1962 (1985).
17. G. Bekefi, R.E. Shefer, and W.W. Destler, Proc. Seventh Int. Free Elec-

tron Laser Conference, Tahoe City, California 1985 (to be published).

18. R.C. Davidson and Y.Z. Yin, Phys. Rev. A30 3078 (1984).

TABLE I. Circular free electron laser parameters for three different wiggler periodicities N as calculated at the "merging points" $k_{\parallel}^{*}$, $\gamma_{\parallel}^{*}$, and ℓ^{*} (see text).

N	R_0 (cm)	$B_{\parallel}$ (kG)	γ_0^{*}	ℓ^{*}	$k_{\parallel}^{*}$ (cm^{-1})	$\omega_r \times 10^{-11}$ (rad sec^{-1})	$\omega_i \times 10^{-9}$ (rad sec^{-1})
6	5.836	0.6817	2.595	57	2.093	3.040	0.4208
12	5.882	0.3918	1.710	22	0.8572	1.426	0.3700
24	5.905	0.2003	1.228	12	0.4546	1.050	0.2972

FIGURE CAPTIONS

Fig. 1. Schematic of the circular free electron laser.

Fig. 2. Axial wave number (a) and instability growth rate (b) as a function of the azimuthal wave number ℓ, for various electron beam energies γ_0; N=6, m=1, a=6.509cm, b=5.398cm, $\omega_{p0} \equiv \left(\frac{4\pi e^2 n_0}{m_0}\right)^{\frac{1}{2}} = 1.50\times10^9 sec^{-1}$, B_W= 0.75kG, $a_0=0.01R_0$, $\Delta/P=0.01$, $(\beta_\theta/\beta_0)^2=0.95$. The heavy dots represent the "tangential interaction points", the asterisk represents the "merging point" (see text).

Fig. 3. Instability growth rate as a function of the azimuthal wave number ℓ, for various electron beam energies γ_0, and a fixed axial wave number $k_{||}=k_{||}^*=2.093cm^{-1}$. $R_0=5.836$. The remaining parameters are the same as those given in the caption to Fig. 2.

Fig. 4. Axial wave number (a) and instability growth rate (b) as a function of the azimuthal wave number ℓ, for different electron ring radii R_0; $\gamma_0=2.60$. The remaining parameters are the same as those given in the caption to Fig. 2.

Fig. 5. The growth rate as a function of electron beam radius R_0; $\gamma_0=2.60$. The remaining parameters are the same as those given in the caption to Fig. 2.

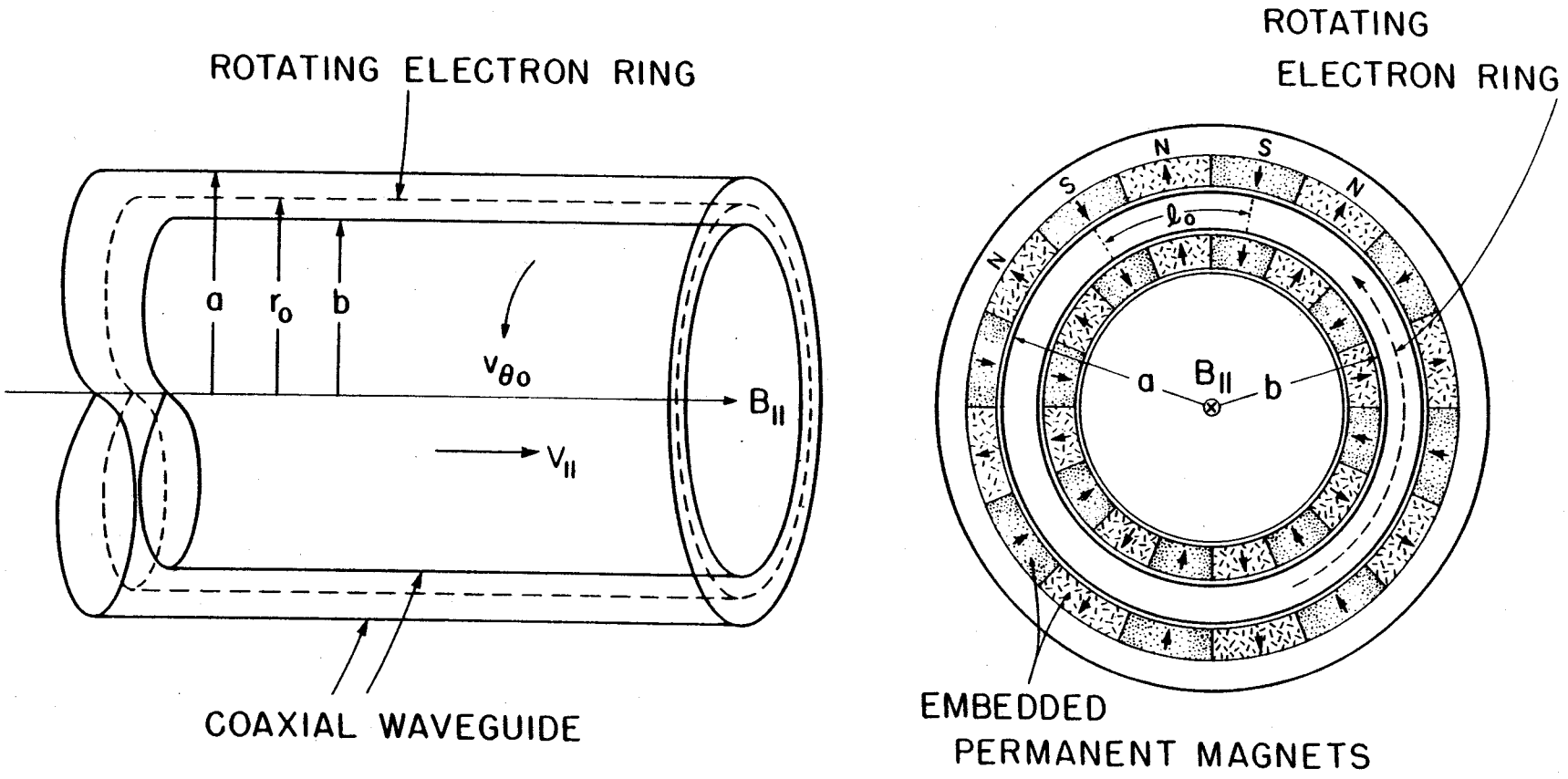

Fig. 1
Yin, Ying, & Bekefi

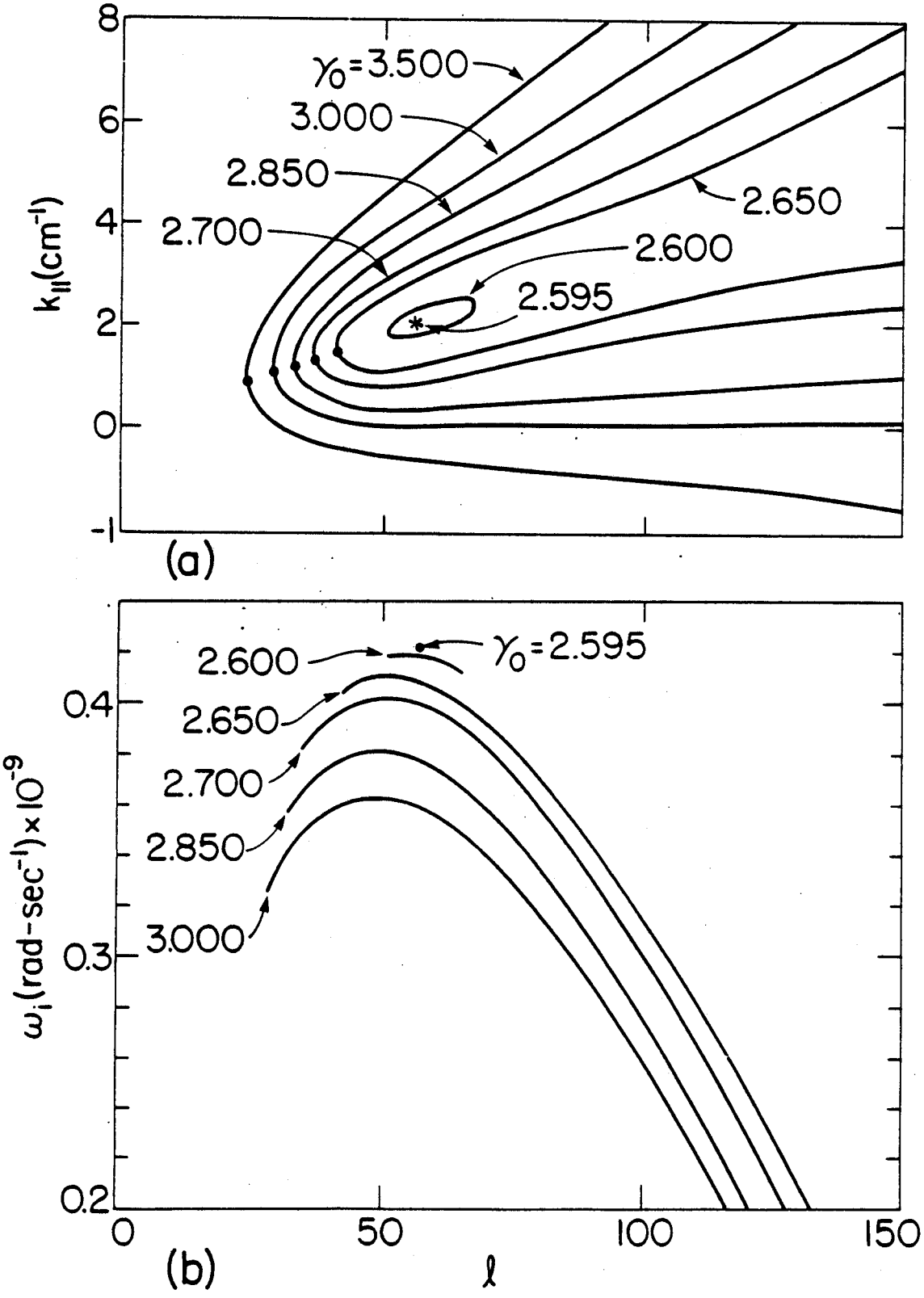

Fig. 2
Yin, Ying, & Bekefi

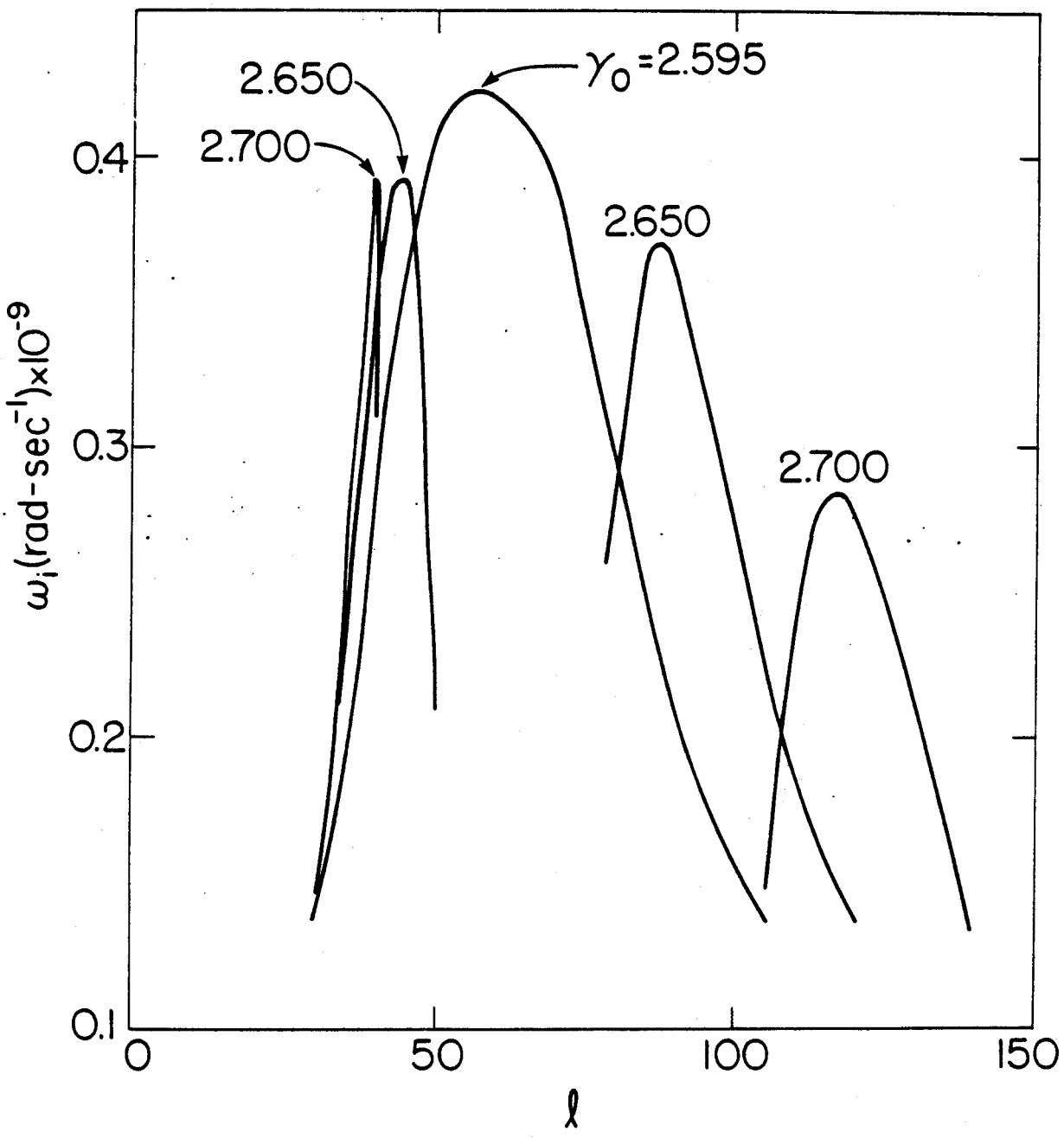

Fig. 3
Yin, Ying, & Bekefi

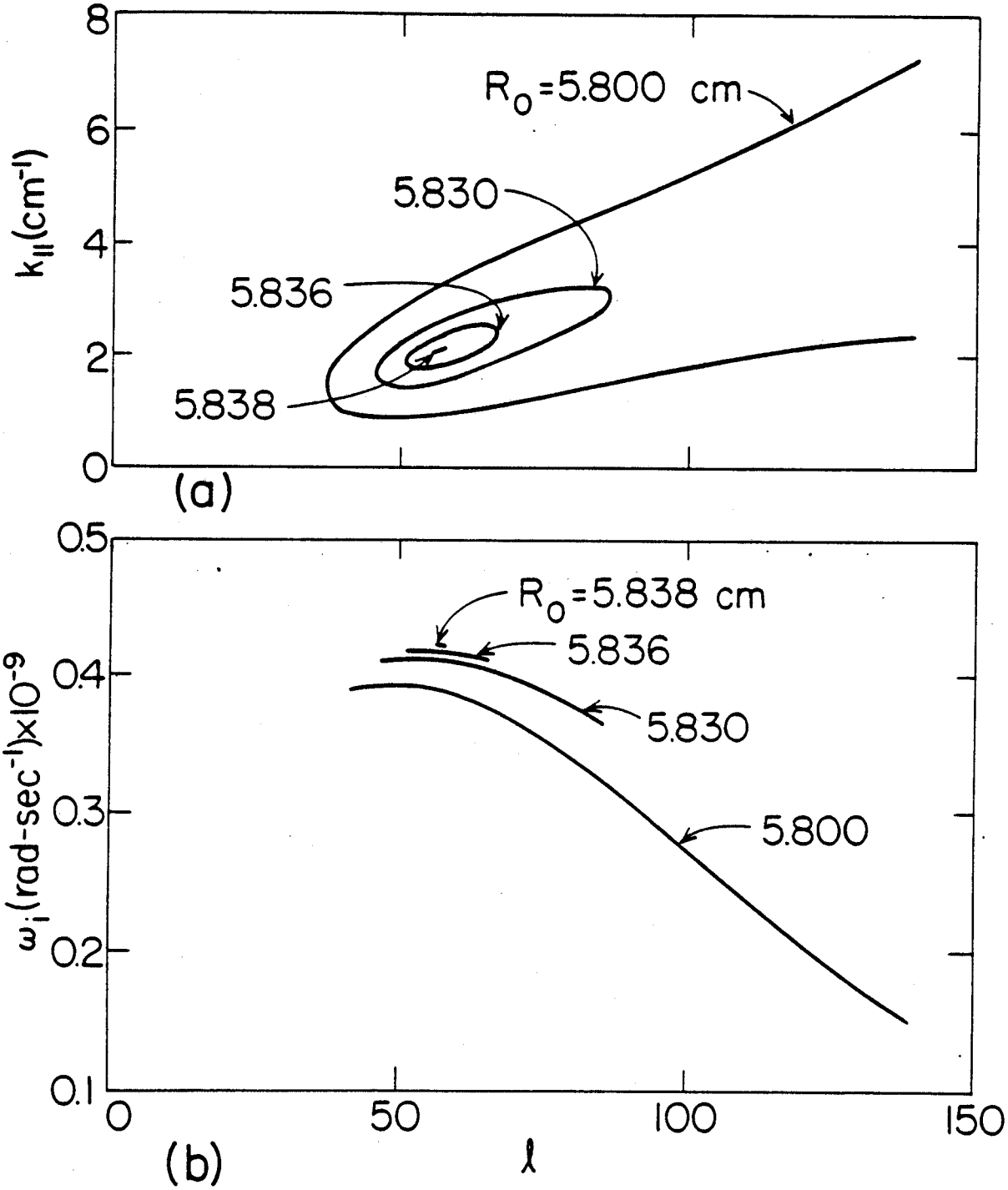

Fig. 4
Yin, Ying, & Bekefi

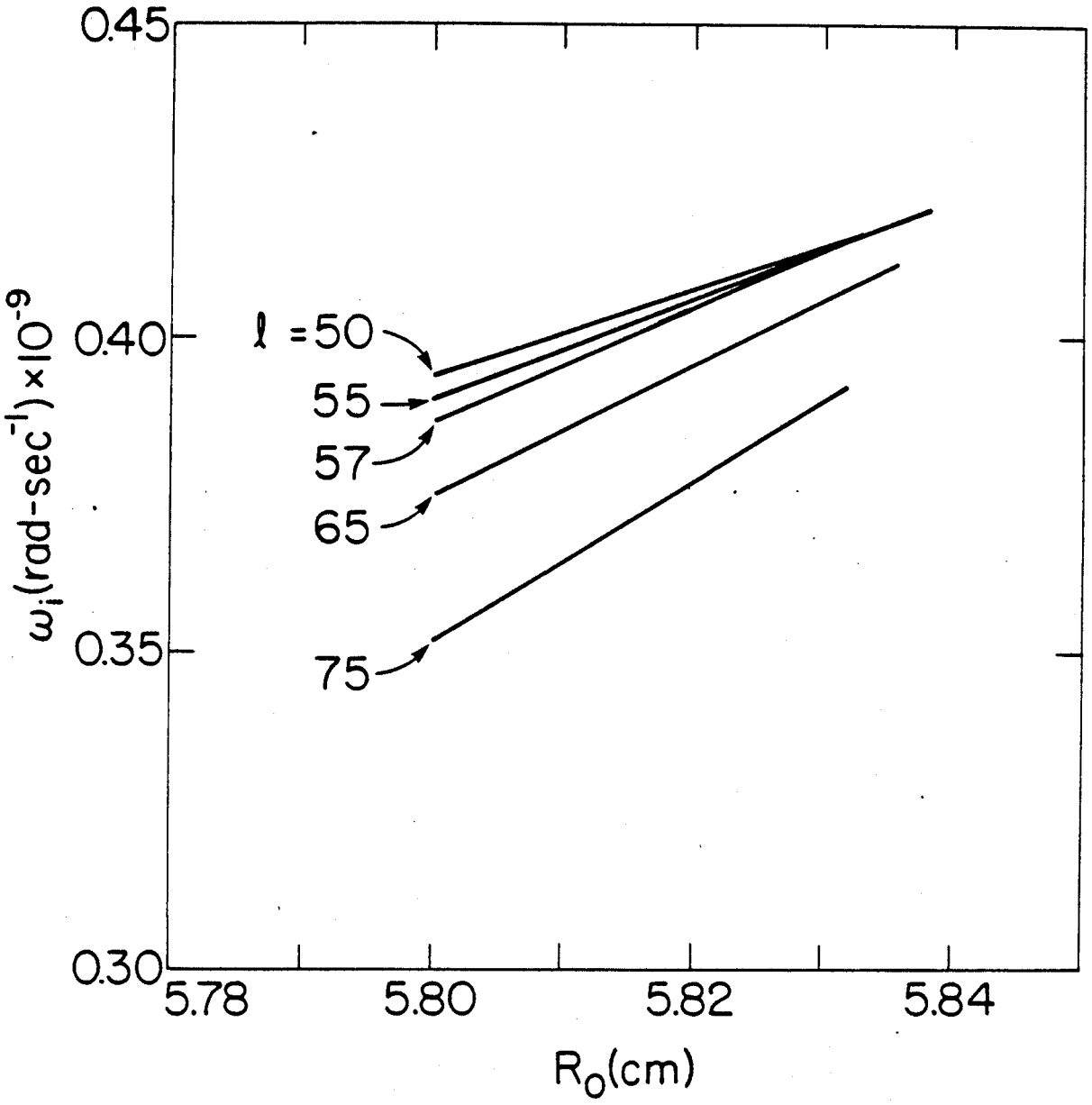

Fig. 5
Yin, Ying, & Bekefi